International Journal of Polymer Analysis and Characterization

ISSN: (Print) (Online) Journal homepage: https://www.tandfonline.com/loi/gpac20

Comprehensive study to ascertain the effect of MnO_2 loading on supercapacitive properties of conducting polymers

Bhagyashri Tale, Kailash Nemade & Pradip Tekade

To cite this article: Bhagyashri Tale, Kailash Nemade & Pradip Tekade (2021): Comprehensive study to ascertain the effect of MnO_2 loading on supercapacitive properties of conducting polymers, International Journal of Polymer Analysis and Characterization, DOI: 10.1080/1023666X.2021.1933853

To link to this article: https://doi.org/10.1080/1023666X.2021.1933853

Published online: 07 Jun 2021.

INTERNATIONAL JOURNAL OF POLYMER ANALYSIS AND CHARACTERIZATION
https://doi.org/10.1080/1023666X.2021.1933853

Taylor & Francis
Taylor & Francis Group

Comprehensive study to ascertain the effect of MnO_2 loading on supercapacitive properties of conducting polymers

Bhagyashri Tale[a], Kailash Nemade[b], and Pradip Tekade[a]

[a]Department of Chemistry, Bajaj College of Science, Wardha, India; [b]Department of Physics, Indira Mahavidyalaya, Kalamb, India

ABSTRACT

This study reports the electrochemical properties of Manganese dioxide (MnO_2) with four types of conducting polymers such as polyaniline (PANi), polythiophene (PTh), polypyyrole, and polyindole (PIn) by preparing their composites. All four conducting polymers were prepared by chemical oxidative polymerization approach. The prepared composites were characterized by X-ray diffraction (XRD), scanning electron microscope (SEM), Raman spectroscopy, ultra–violate visible (UV–VIS) spectroscopy, and photoluminance (PL). Similarly, the supercapacitive properties such, cyclic voltammetry (CV) curve, capacitance retention and cycle stability of composite materials were investigated. The highest value of specific capacitance was obtained for MnO_2-PANi (Mn-PANi) composite, which was found to be 633.75 Fg^{-1}.

ARTICLE HISTORY
Received 2 December 2020
Accepted 19 May 2021

KEYWORDS
Conducting polymers; MnO_2; supercapacitor

Introduction

Global demand of energy is increasing day by day. As demand of high energy storage system is increased globally, study of electrode material for supercapacitor application became topic of intense research. Climate changes and the limited availability of fossil fuels create a need of sustainable and renewable energy sources. Thus, renewable energy production from sun and wind, as well as the development of electric/hybrid electric vehicles with low CO_2 emissions has started. As the sun does not shine during the night and wind does not blow on demand, energy storage systems play a major role and electrical energy storage systems, such as batteries, electrochemical capacitors (ECs) are need to be developed. The performance of energy storage systems has to be increased substantially to meet the higher requirements of future systems. ECs (also known as supercapacitors or ultracapacitors) store energy by ion adsorption (electrochemical double-layer capacitors) or fast surface redox reactions (pseudo-capacitors). These can be more efficient than batteries used in electrical energy storage, when high power delivery or uptake is needed. Numerous efforts have been taken to increase the specific capacitance value of the electrode materials. The electrode materials with high capacity and cyclic stability found to possess great supercapacitor performance.[1–3]

Over the past decades, various types of electrode materials are studied for high-performance supercapacitor application and many approaches are employed to fabricate various composites prepared using different types of electroactive materials. As lithium-ion batteries has some disadvantages such as slow power delivery or uptake, faster and higher power energy storage systems are needed and for this, supercapacitor are considered as good alternative. ECs are power devices

CONTACT Bhagyashri Tale bhagyashritale@gmail.com Department of Chemistry, Bajaj College of Science, Wardha, Maharashtra, India.

which can be fully charged or discharged in seconds. Their energy density (about 5 Wh kg^{-1}) is lower as compared to batteries, but it shows much higher power delivery or uptake (10 kW kg^{-1}) for shorter times (a few seconds). They can replace batteries in the energy storage field for uninterruptible power supplies (back-up supplies used to protect against power disruption) and load-leveling.[4–6]

Transition metal oxides and conducting polymers are pseudo-capacitive active materials. Addition of metal oxides to conducting polymers is called composites. Composite formation improves electrochemical properties. Among transition metal oxides, manganese dioxide (MnO_2) shows best EC properties than others. PANi/MnO_2 composite has been studied by Chen et al who reported the specific capacitance value of 80 F g^{-1} and its stable columbic efficiency of about 98% up to 1000 cycles.[2]

Transition metal oxides such as RuO_2,[7] NiO,[8,9] CoOx, and MnO_2[10] are studied and implemented as electrode materials for SCs.[11–15] Metal oxides have wide charge/discharge potential range, but most of the transition metal oxides shows relatively low capacitance.[11,14] Conducting polymers such as polyaniline (PANi) are reported as another promising material in the redox SCs. Polymers shows advantages such as high capacitance, high conductivity, low cost, and ease of fabrication.[16] But they suffer from disadvantages such as the relatively low mechanical stability and cycle life which are major limitations for applications. In recent years, considerable efforts have been made to couple the unique advantages of these capacitive materials for SCs by formation of composites.[17–22] Thus, the composites of PANi and MnO_2 have attracted much attention because of their low cost and eco-friendliness. The PANi-MnO_2 composite can be prepared using different chemical methods.[18,23–28] The PANi serves as an electroactive material for energy storage and it is also a good coating layer to protect MnO_2 from dissolution in acidic electrolytes.[23] It is reported that the composite prepared by intercalation of PANi into layers of MnO_2 shows an enhanced specific capacitance of 330 $F.g^{-1}$ by the synergistic effects.[24]

Motivating from above discussion, we planned to investigate the electrochemical properties of MnO_2 with four types of conducting polymers such as PANi, polythiophene (PTh), polypyyrole, and polyindole (PIn) by preparing their composites. In this work, we studied the supercapacitive properties such, cyclic voltammetry (CV) curve, capacitance retention, and cycle stability performance of composite materials. Prime novelty of present work is that out of four type of composites system of MnO_2 with conducting polymer, we successfully optimized MnO_2-PANi (Mn-PANi) composite system as active electrode material for supercapacitor application.

Experimental

In this work, chemicals of analytical grade procured from SD Fine, India of purity 99.8% were used without further purification. PANi was synthesized with chemical oxidative method using ammonium persulfate as oxidizing agent. Both aniline and oxidant in 1:1 ratio were dissolved in aqueous medium. The greenish black ppt was observed and it was kept for 24 h at room temperature in order to get complete polymerization. The obtained product was washed with distilled water and dried in an oven.[29] For polymerization of pyrrole, $FeCl_3$ was used as oxidant and ethanol as solvent. The suspension was kept at room temperature for 24 h for polymerization. Finally, solution was filtered and washed with acetone and distilled water to remove unreacted pyrrole and excess ferric chloride. A black ppt of polypyrrole (PPy) was dried in an oven.[30]

PIn was prepared *via* chemical oxidative technique using $FeCl_3$ as an oxidant. In this technique, monomer and oxidant in stoichiometric ratio were dissolved in distilled water. To that reaction mixture, 0.1 M hydrogen peroxide was added to enhance the rate of reaction. The reaction mixture was continuously stirred for 12 h with magnetic stirrer at 30 °C.[31] PTh was synthesized at room temperature by mixing thiophene with ferric chloride in distilled water. Hydrogen peroxide was added dropwise to reaction mixture to enhance the rate of reaction. The

polymerization was allowed to take place with constant stirring for 24 h with magnetic stirring at 30°. Then concentrate sodium hydroxide solution was added to generate precipitate. The precipitate was washed with distilled water and dried in oven.[32]

MnO_2 was synthesized using co-precipitation method using manganese sulfate monohydrate ($MnSO_4.H_2O$) and potassium permanganate ($KMnO_4$). The solution was further stirred for 20 min and kept at room temp. for 24 h. The solution was probe sonicated using sonicator (PCi, 750-F, PCI analytics Pvt. Ltd) to split the MnO_2 particles to nano dimensions. The black-brown product was obtained which is washed with deionized water and dried in oven.[33] The *ex-situ* approach was adopted for preparation of polymer/metal oxide composite. The weight % stoichiometry was adopted for preparation of composite. During preparation of composite, polymer (1 g) and metal oxide (0.1 g) was added in organic media.

The X-ray diffraction (XRD) patterns of as prepared materials were recorded on Rigaku Miniflex-II X-ray diffractometer. The morphology of samples was investigated using scanning electron microscope (SEM) images obtained from JEOL JSM-7500F. The ultraviolet–visible (UV–VIS) absorption spectra of composites were acquired using Agilent Cary 60 UV–VIS spectrophotometer. The Bruker RFS 27 Raman spectrometer was used for Raman analysis. Electrochemical study of prepared samples was carried out using three-electrode cell systems (CHI 660D, CHInstruments). As-prepared materials were used as the working electrode, platinum wire as counter electrode and Ag/AgCl as the reference electrode. In this work, the working electrodes were prepared by mixing 85 wt.% sample that is Mn-PANi composite, 10 wt.% activated carbon, and 5 wt% polytetrafluoroethylene with acetone. Then the mixture of sample was coated onto a nickel foam using spin coating technique. Photoluminescence (PL) spectra recorded using fluorescence spectroscopy (FL spectrophotometer model F-7000; Hitachi).

Results and discussion

The XRD patterns of the MnO_2 micromaterials are shown in Figure 1(a–i). The diffraction peak which appeared at $2\theta = 18°$, 28°, 37°, 42°, 56° matched well with the diffraction peak of α- MnO_2 standard data (JCPDS card PDF file no. 44-0141).[34] XRD of PANi recorded at room temperature with several diffraction peaks in the 2θ range 15–30°. The pattern shows sharp and well-defined peaks, which indicate semi-crystalline nature of PANi. The crystalline nature of PANi is due to its nano fibrous form and planer nature of benzenoid and quinoid functional groups.[35]

XRD spectra of PTh shows only one broad peak centered at near 2θ value of 35°. This diffraction peak strongly associated with the π-π stacking structure in PTh chains. Thus, spectrum shows that the semi-crystalline nature of PTh.[36] The XRD pattern of PIn showing a broad hump which suggests an amorphous structure which is the characteristic of PIn.[31] It is observed from the XRD of PPy that the polymer is in an amorphous state, and hence there are no sharp peaks observed in the diffraction pattern. But a broad peak at about 24° of 2θ value is observed, which incidentally is the characteristics peak of amorphous PPy polymer.[37]

The XRD pattern of Mn-PANi composite clearly shows the crystalline phase with shape peaks. The XRD patterns of MnO_2-PIn composite (Mn-PIn), MnO_2-PPy composite (Mn-PPy), and MnO_2-PTh composite (Mn-PTh) indicates amorphous nature as there is no sharp peak. Table 1 shows the particle size estimated from XRD analysis.

Figure 2(a–i) shows the SEM images of (a) MnO_2, (b) PANi, (c) PTh, (d) PPy, (e) PIn, (f) MnO_2-PANi, (g) MnO_2-PTh, (h) MnO_2-PPy, and (i) MnO_2-PIn, respectively. SEM images shows the good quality information about the surface topography of as-prepared materials.

Raman spectra of MnO_2 clearly showing sharp peaks in the region between 500 and 700 cm^{-1}, which is characteristic peak of MnO_2 (Figure 3).[39] Raman spectra of PANi clearly indicate signal at 1140, 1230, 1500, and 1582 cm^{-1}. The 1100–1210 cm^{-1} region indicates C–H bending vibrations of benzene or quinone type rings. The 1210–1520 cm^{-1} region denotes C-N stretching

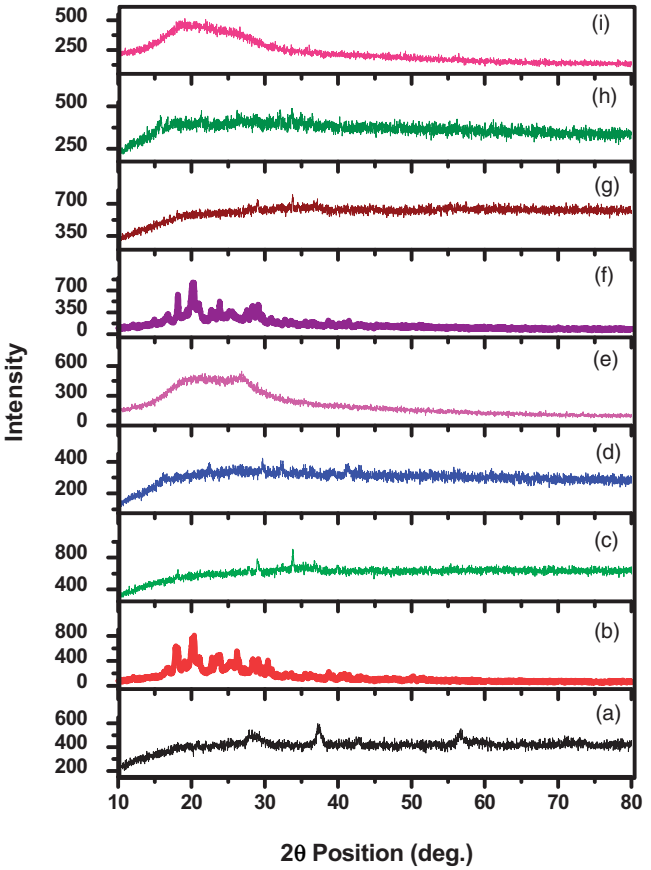

Figure 1. XRD patterns of (a) MnO_2, (b) PANi, (c) PTh, (d) PPy, (e) PIn, (f) MnO_2-PANi, (g) MnO_2-PTh, (h) MnO_2-PPy, and (i) MnO_2-PIn.

Table 1. Particle size of MnO_2, polymers, and their composites.

Compound	Estimated particle size by Scherrer equation D(nm)= $K\lambda/\beta Cos\theta$ (nm) [38]
MnO_2	61.32
Polyaniline (PANi)	84
Polythiophene (PTh)	108.51
Polypyrrole (PPy)	108.13
Polyindole (PIn)	10.28
MnO_2-polyaniline composite (Mn-PANi)	90.16
MnO_2-polythiophene composite (Mn-PTh)	132.87
MnO_2-polypyrrole composite (Mn-PPy)	91.23
MnO_2-polyindole composite (Mn-PIn).	7.20

vibrations and 1520–1650 cm^{-1} region represents C–C stretching vibration of benzene and quinone type rings.[40]

PTh shows sharp peak at 1209, 1379, and 1651 cm^{-1}. Signal near 1600 cm^{-1} shows unquestionably frequency dispersion with increasing chain length. Peak near1500 cm^{-1} is a common feature of/the Raman spectra of aromatic and heteroaromatic systems. It is always very strong and dominates the whole Raman spectrum. While it shifts to lower frequencies when chain length increases. It shows somewhat different frequencies from one chemical series to another within the class of oligo and PThs, but within each class it is almost invariably strong and unshifted. Some signals which appear at the lower frequency side shows intensity enhancement with increasing

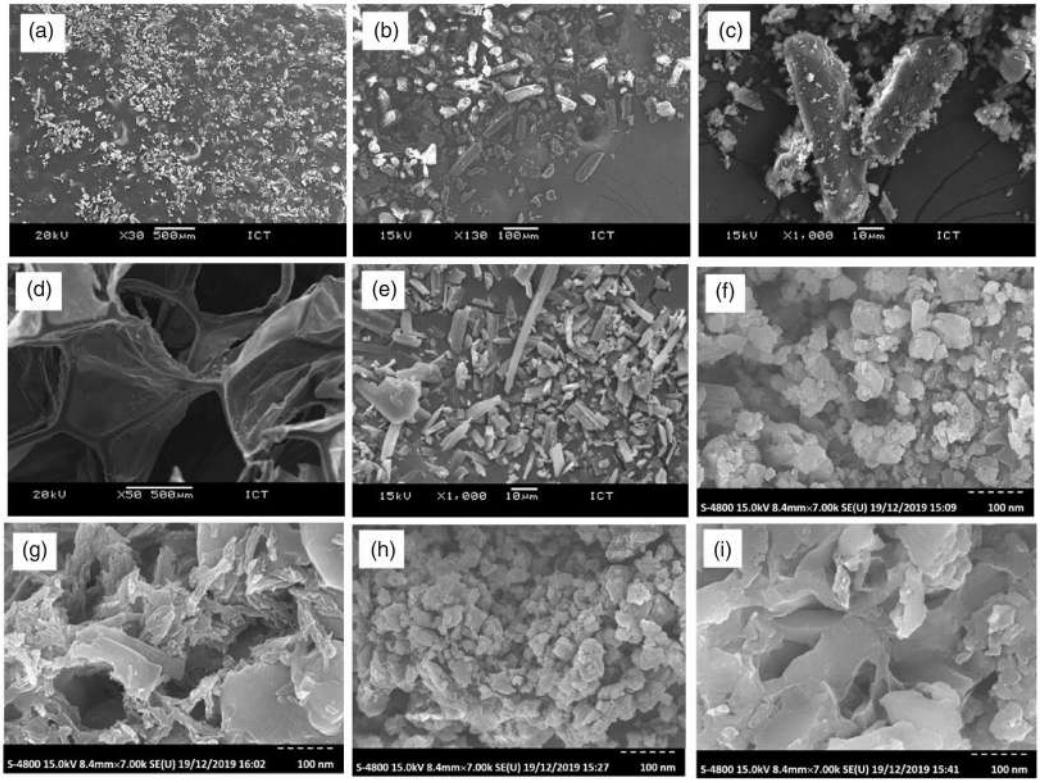

Figure 2. SEM images of (a) MnO_2, (b) PANi, (c) PTh, (d) PPy, (e) PIn, (f) MnO_2-PANi, (g) MnO_2-PTh, (h) MnO_2-PPy, and (i) MnO_2-PIn.

chain length.[41] PPy shows signal at 1330 cm^{-1} which corresponds to C–C stretching in ring and antisymmetric C–N stretching.[42] PIn shows signal 1102 due to out-of-plane as well as in-plane deformation of N-H, peak near 1594 corresponds to C = C backbone stretching and peak at 1414 due to ring stretching.[43,44]

In this work, UV–VIS technique was used to know the absorption wavelengths of materials and band gap (Figure 4). The energy band gap of sample can be calculated using relations: $E = hc/\lambda$,[45] where, Energy (E) = Band gap, Planks constant (h)=6.626×10^{-34} J s, Velocity of Light (c) = 2.99×10^8 m/s, and Wavelength (λ) = Absorption peak value. 1 eV = 1.6×10^{-19} J (Conversion factor). Table 2 shows the band gap values of as-prepared materials.

In PL spectra, MnO_2 signal is found to in range of 300–800 nm (Figure 5). The spectrum exhibits prominent emission bands located in green–violet spectral region. A broad weak emission in the green region is observed at around 520 nm which can be ascribed to the surface defects or surface dangling bonds.[46–48] PANi shows peak at 367 nm, due to $\pi \rightarrow \pi^*$ transition.[49] PTh shows absorption near excitation wavelength 325 nm.[50] PL signal for PIn can be observed which comes from the recombination of electron in singly occupied oxygen vacancies with photo exited holes.[51–53] PPy shows PL emission peaks near 400 nm. However, agglomeration affects the PL intensity of the polymer.[51] This PL emission characteristics demonstrate the promise of the synthesized materials for practical applications in ultraviolet and visible light emission devices.

Figure 6 shows the cyclic voltammetric (CV) curves of MnO_2, PANi, PTh, PPy, PIn, Mn-PANi, MnO_2-PTh, MnO_2-PPy, and MnO_2-PIn recorded at a scan rate of 50 mV s^{-1}. The CV curves clearly shows that prepared composite has higher supercapacitive properties than sperate MnO_2, PANi, PTh, PPy, and PIn. The superior supercapacitive properties of composite attributed

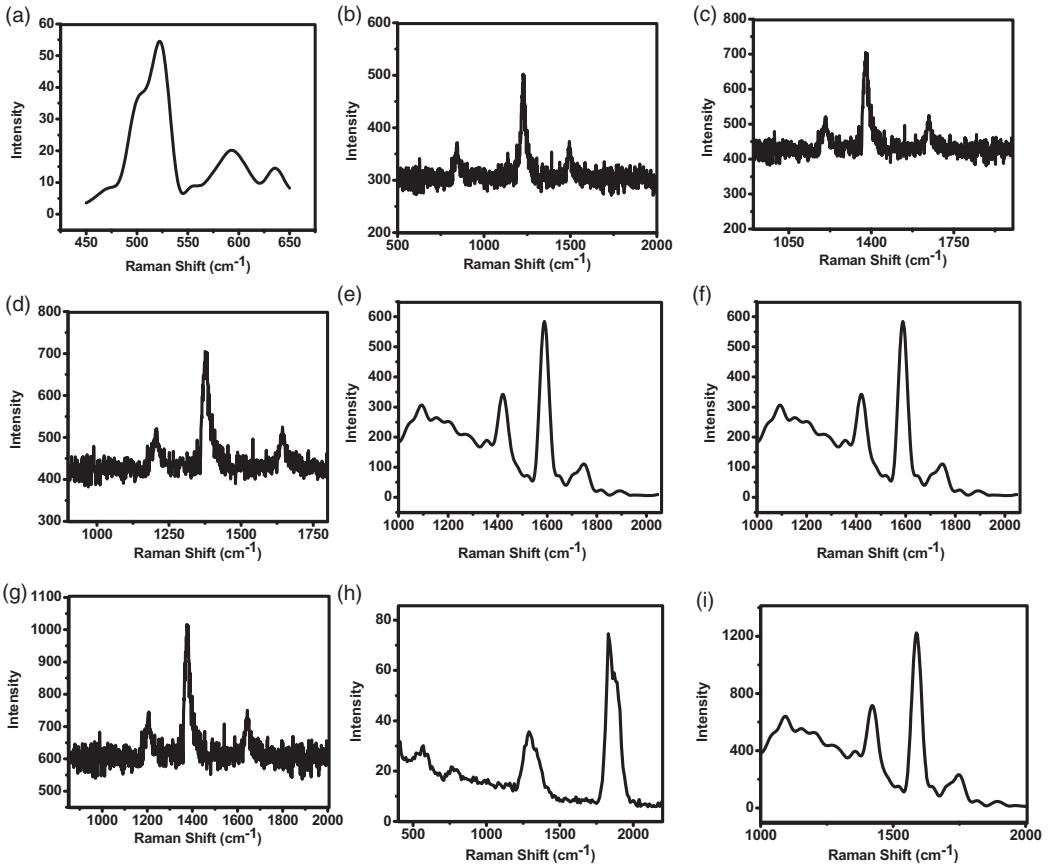

Figure 3. Raman Spectra of (a) MnO_2, (b) PANi, (c) PTh, (d) PPy, (e) PIn, (f) MnO_2-PANi, (g) MnO_2-PTh, (h) MnO_2-PPy, and (i) MnO_2-PIn.

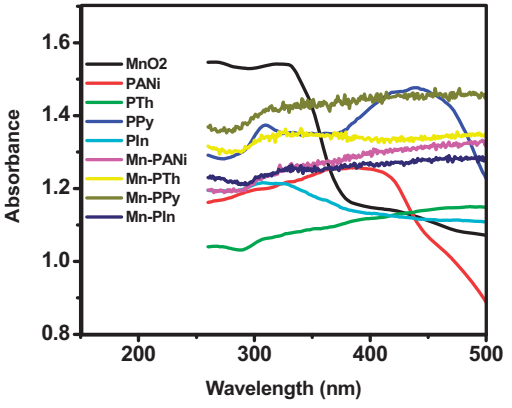

Figure 4. UV–VIS spectra of MnO_2, PANi, PTh, PPy, PIn, MnO_2-PANi, MnO_2-PTh, MnO_2-PPy, and MnO_2-PIn.

to synergetic effect between conducting polymers and MnO_2. Specific capacitance has been estimated using the relation (Equation (1))[45]

$$Cs = \frac{I}{m \times v}(Fg^{-1}) \tag{1}$$

Table 2. Band gap and Absorption peak values for MnO_2, Polymers and their composites.

Compound	Absorption peak value (nm)	Band gap (eV)
1. MnO_2	410	3.02
2. Polyaniline (PANi)	310	3.99
3. Polythiophene (PTh)	265	4.67
4. Polypyrrole (PPy)	440	2.82
5. Polyindole (PIn)	249	4.98
6. MnO_2-Polyaniline composite (Mn-PANi)	241	5.14
7. MnO_2-Polythiophene composite (Mn-PTh)	339	3.66
8. MnO_2-Polypyrrole composite (Mn-PPy)	394	3.15
9. MnO_2-Polyindole composite (Mn-PIn)	250	4.95

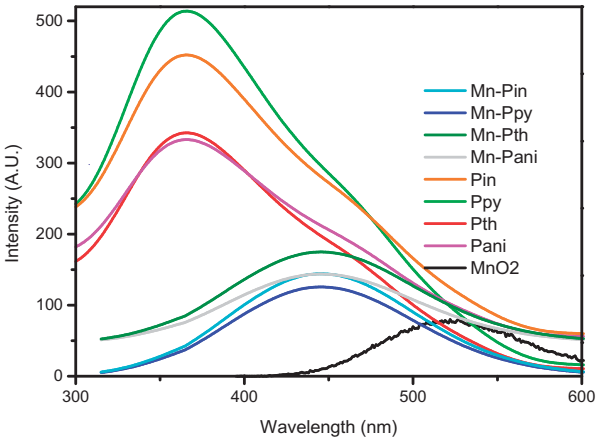

Figure 5. PL spectra of MnO_2, PANi, PTh, PPy, PIn, MnO_2-PANi, MnO_2-PTh, MnO_2-PPy, and MnO_2-PIn.

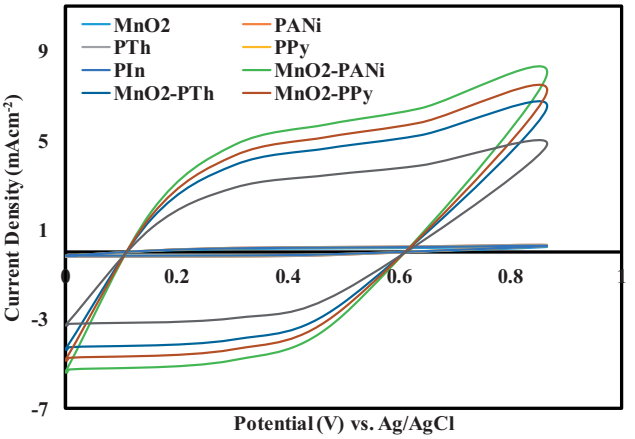

Figure 6. CV curves of MnO_2, PANi, PTh, PPy, PIn, MnO_2-PANi, MnO_2-PTh, MnO_2-PPy, and MnO_2-PIn recorded at a scan rate of 50 $mV.s^{-1}$.

where I is the average current during anodic and cathodic scan (A), m is the mass of the electrode (g), and v is the scan rate (V). In our case, the highest value of specific capacitance was associate with Mn-PANi composite, which was found to be 633.75 Fg^{-1} at a scan rate of 50 mV s^{-1}. The significant enhancement in electrochemical performance was attributed to improved carrier density, which results in good electrical conductivity.[54] Further study, confined about Mn-PANi composite, as it is optimized sample in this study.

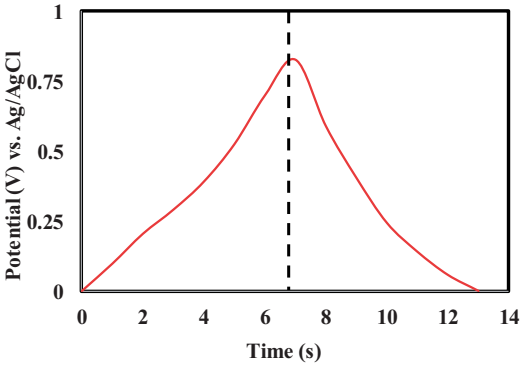

Figure 7. Galvanostatic charge/discharge curves of the MnO_2-PANi composite collected at a current density of 10 μAcm^{-2}.

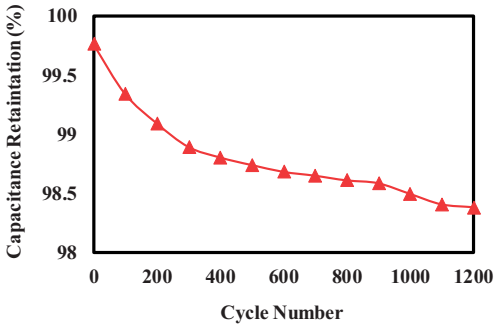

Figure 8. Cycle performance of the MnO_2-PANi composite measured at a scan rate of 50 mV s^{-1} for 1200 cycles.

Table 3. Comparison of present work with some recent reports on supercapacitive properties of MnO2-PANi composites.

Electrode material	Method	Specific capacitance (Fg^{-1})	References
Polyaniline–MnO_2 nanotube hybrid nanocomposite	*In situ* polymerization	626	[56]
MnO_2 nanorods intercalating graphene oxide/ polyaniline ternary composites	*Ex-situ* approach	512	[57]
Ultralong manganese dioxide/polyaniline coaxial nanowires	*Ex-situ* approach	346	[58]
MnO_2-PANi composite	*Ex-situ* approach	633.75	This work

Figure 7 shows the galvanostatic charge/discharge (GCD) curves of Mn-PANi composite. The GCD curves of Mn-PANi composite is nearly symmetric. As expected, Figure 7 shows that the Mn-PANi composite based electrode shows longer discharge time. It is due to the highest specific capacitance associated with Mn-PANi composite. Better electrochemical performance of Mn-PANi composite accredited to synergetic effect between MnO_2 and PANi.

Figure 8 depicts the capacitance drops in Mn-PANi composite. The Mn-PANi composite exhibits good stability with ∼98.28% capacitance retention after 1200 cycles. Stable performance of Mn-PANi composite is ascribed to enhanced electrical conductivity and highly stable surface redox reaction.[55]

Table 3 shows the recent reports on supercapacitive properties of Mn-PANi composites and their comparison with findings of this work.

Conclusions

In this work, we successfully prepared the composites of MnO_2 and PANi, PTh, PPy, and PIn and mainly studied their supercapacitive properties. Similarly, the composites were characterized by XRD, SEM, Raman spectroscopy, UV–VIS spectroscopy, and PL. The highest value of specific capacitance was associate with Mn-PANi composite, which was found to be 633.75 Fg^{-1} at a scan rate of 50 $mV.s^{-1}$. The main accomplishment of this study is that MnO_2-PANi composite shows stable performance up to 1200 cycles.

Acknowledgments

The authors are very much thankful to Principal, Bajaj College of Science, Wardha, India for providing necessary facilities for the work.

References

[1] Chen, S. M., R. Ramachandran, V. Maniand, and R. Saraswathi. 2014. Recent advancements in electrode materials for the high-performance electrochemical supercapacitors: a review. *Int. J. Electrochem. Sci.* 9: 4072–4085.

[2] Chen, L., L. J. Sun, F. Luan, Y. Liang, Y. Li, and X. X. Liu. 2010. Synthesis and pseudocapacitive studies of composite films of polyaniline and manganese oxide nanoparticles. *J. Power Sources* 195:3742–3747. doi:10.1016/j.jpowsour.2009.12.036

[3] SimonandY. Gogotsi, P. 2010. Materials for electrochemical capacitors. *In Nanoscience and Technology: A Collection of Reviews from Nature Journals, pp.* 320–329. Singapore: World Scientific.

[4] Conwa, B. E . 1999. *Electrochemical Supercapacitors, Scientific Fundamentals and Technological Applications*. 2nd ed. New York, NY: Kluwer Academic/Plenum Press.

[5] Conwa, B. E. 2013. *Electrochemical Supercapacitors: Scientific Fundamentals and Technological Applications*. Berlin, Germany: Springer Science and Business Media.

[6] Miller, J. R., and P. Simon. 2008. Materials science. Electrochemical capacitors for energy management. *Science* 321:651–652. doi:10.1126/science.1158736

[7] Hu, C. C., K. H. Chang, M. C. Lin, and Y. T. Wu. 2006. Design and tailoring of the nanotubular arrayed architecture of hydrous RuO2 for next generation supercapacitors. *Nano Lett.* 6:2690–2695. doi:10.1021/nl061576a

[8] Yuan, C., X. Zhang, L. Su, B. Gao, and L. Shen. 2009. Facile synthesis and self-assembly of hierarchical porous NiO nano/micro spherical superstructures for high performance supercapacitors. *J. Mater. Chem.* 19: 5772–5777. doi:10.1039/b902221j

[9] Liu, K. C., and M. A. Anderson. 1996. Porous nickel oxide/nickel films for electrochemical capacitors. *J. Electrochem. Soc.* 143:124–130. doi:10.1149/1.1836396

[10] Sun, L. J., X. X. Liu, K. K. T. Lau, L. Chen, and W. M. Gu. 2008. Electrodeposited hybrid films of polyaniline and manganese oxide in nanofibrous structures for electrochemical supercapacitor. *Electrochim. Acta* 53:3036–3042. doi:10.1016/j.electacta.2007.11.034

[11] Beaudrouet, E., A. Le Gal La Salle, and D. Guyomard. 2009. Nanostructured manganese dioxides: synthesis and properties as supercapacitor electrode materials. *Electrochim. Acta* 54:1240–1248. doi:10.1016/j.electacta.2008.08.072

[12] Wang, Y. G., and Y. Y. Xia. 2006. Electrochemical capacitance characterization of NiO with ordered mesoporous structure synthesized by template SBA-15. *Electrochim. Acta* 51:3223–3227. doi:10.1016/j.electacta.2005.09.013

[13] Wei, T. Y., C. H. Chen, K. H. Chang, S. Y. Lu, and C. C. Hu. 2009. Cobalt oxide aerogels of ideal supercapacitive properties prepared with an epoxide synthetic route. *Chem. Mater.* 21:3228–3233. doi:10.1021/cm9007365

[14] Yu, P., X. Zhang, D. Wang, L. Wang, and Y. Ma. 2009. Shape-controlled synthesis of 3D hierarchical MnO2 nanostructures for electrochemical supercapacitors. *Cryst. Growth Des.* 9:528–533. doi:10.1021/cg800834g

[15] Zheng, J. P., and T. R. Jow. 1996. High energy and high-power density electrochemical capacitors. *J. Power Sources* 62:155–159. doi:10.1016/S0378-7753(96)02424-X

[16] Li, H., J. Wang, Q. Chu, Z. Wang, F. Zhang, and S. Wang. 2009. Theoretical and experimental specific capacitance of polyaniline in sulfuric acid. *J. Power Sources* 190:578–586. doi:10.1016/j.jpowsour.2009.01.052

[17] Yuan, A., and Q. Zhang. 2006. Novel hybrid manganese dioxide/activated carbon supercapacitor using lithium hydroxide electrolyte. *Electrochem. Commun.* 8:1173–1178. doi:10.1016/j.elecom.2006.05.018
[18] Bian, C., A. Yu, and H. Wu. 2009. Fibriform polyaniline/nano-TiO2 composite as an electrode material for aqueous redox supercapacitors. *Electrochem. Commun.* 11:266–269. doi:10.1016/j.elecom.2008.11.026
[19] Kim, J. H., A. K. Sharma, and Y. S. Lee. 2006. Synthesis of polypyrrole and carbon nano-fiber composite for the electrode of electrochemical capacitors. *Mater. Lett.* 60:1697–1701. doi:10.1016/j.matlet.2005.12.002
[20] Yan, J., Z. Fan, T. Wei, J. Cheng, B. Shao, K. Wang, L. Song, and M. Zhang. 2009. Carbon nanotube/MnO2 composites synthesized by microwave-assisted method for supercapacitors with high power and energy densities. *J. Power Sources* 194:1202–1207. doi:10.1016/j.jpowsour.2009.06.006
[21] Barpanda, P., Y. Li, F. Cosandey, S. Rangan, R. A. Bartynski, and G. G. Amatucci. 2009. Amatucci, fabrication, physical and electrochemical investigation of microporous carbon polyiodide nanocomposites. *J. Electrochem. Soc.* 156:A873–A885. doi:10.1149/1.3212851
[22] Zhu, S., W. Cen, L. Hao, J. Ma, L. Yu, H. Zheng, and Y. Zhang. 2014. Flower-like MnO2 decorated activated multihole carbon as high-performance asymmetric supercapacitor electrodes. *Mater. Lett.* 135:11–14. doi:10.1016/j.matlet.2014.07.120
[23] Yuan, C., L. Su, B. Gao, and X. Zhang. 2008. Enhanced electrochemical stability and charge storage of MnO2/carbon nanotubes composite modified by polyaniline coating layer in acidic electrolytes. *Electrochim. Acta* 53:7039–7047. doi:10.1016/j.electacta.2008.05.037
[24] Zhang, X., L. Ji, S. Zhang, and W. Yang. 2007. Synthesis of a novel polyaniline-intercalated layered manganese oxide nanocomposite as electrode material for electrochemical capacitor. *J. Power Sources* 173: 1017–1023. doi:10.1016/j.jpowsour.2007.08.083
[25] Sun, L. J., and X. X. Liu. 2008. Electrodepositions and capacitive properties of hybrid films of polyaniline and manganese dioxide with fibrous morphologies. *Eur. Polym. J.* 44:219–224. doi:10.1016/j.eurpolymj.2007.10.017
[26] Liu, F. J., T. F. Hsu, and C. H. Yang. 2009. Construction of composite electrodes comprising manganese dioxide nanoparticles distributed in polyaniline–poly (4-styrene sulfonic acid-co-maleic acid) for electrochemical supercapacitor. *J. Power Sources* 191:678–683. doi:10.1016/j.jpowsour.2009.02.046
[27] Liu, F. J. 2008. Electrodeposition of manganese dioxide in three-dimensional poly (3, 4-ethylenedioxythiophene)–poly (styrene sulfonic acid)–polyaniline for supercapacitor. *J. Power Sources* 182:383–388. doi:10.1016/j.jpowsour.2008.04.008
[28] Prasad, K. R., and N. Miura. 2004. Polyaniline-MnO2 composite electrode for high energy density electrochemical capacitor. *Electrochem. Solid-State Lett.* 7:A425. doi:10.1149/1.1805504
[29] Jing, X., Y. Wang, D. Wu, and J. Qiang. 2007. Sonochemical synthesis of polyaniline nanofibers. *Ultrason. Sonochem.* 14:75–80. doi:10.1016/j.ultsonch.2006.02.001
[30] Vernitskaya, T. V., and O. N. Efimov. 1997. Polypyrrole: a conducting polymer; its synthesis, properties and applications. *Russ. Chem. Rev.* 66:443–457. doi:10.1070/RC1997v066n05ABEH000261
[31] Wadatkar, N. S., and S. A. Waghuley. 2015. Complex optical studies on conducting polyindole as-synthesized through chemical route. *Egyptian J. Basic Appl. Sci.* 2:19–24. doi:10.1016/j.ejbas.2014.12.006
[32] Wadatkar, N. S., and S. A. Waghuley. 2016. Studies on properties of as-synthesized conducting polythiophene through aqueous chemical route. *J. Mater. Sci. Mater. Electron.* 27:10573–10581. doi:10.1007/s10854-016-5152-7
[33] hi Hong hanhNguyen. 2017. Synthesis of MnO2 nanoparticle catalyst and application to treatment of organic compounds in agricultural processing villages- a case study in duong lieu village, ha noi Capital, Vietnam. *Int. J. Agric. Innov. Res.* 6:103–107.
[34] Nemade, K. R., and S. A. Waghuley. 2014. Preparation of MnO2 immobilized graphene nanocomposite by solid state diffusion route for LPG sensing. *J. Lumin.* 153:194–197. doi:10.1016/j.jlumin.2014.03.039
[35] Bhagwat, A. D., S. S. Sawantand and C. M. Mahajan. 2016. Facile rapid synthesis of polyaniline (PANI) nanofibers. *J. Nano- Electron. Phys.* 8: 01037.
[36] Sakthiveland, S., and A. Boopathi. 2014. Synthesis and preparation of polythiophene thin film by sPIn coating method. *Int. J. Sci. Res. sec* 141:97–100.
[37] Ma, C., P. Sg, G. Pr, and S. Shashwati. 2011. Synthesis and characterization of polypyrrole (PPy) thin films. *Soft Nanosci. Lett.* 1:6–10.
[38] Nemade, K. R., and S. A. Waghuley. 2014. Low temperature synthesis of semiconducting α-Al2O3 quantum dots. *Ceram. Int.* 40:6109–6113. doi:10.1016/j.ceramint.2013.11.062
[39] Wei, M., Y. Konishi, H. Zhou, H. Sugihara, and H. Arakawa. 2005. Synthesis of single-crystal manganese dioxide nanowires by a soft chemical process. *Nanotechnology* 16:245–249. doi:10.1088/0957-4484/16/2/011
[40] Mažeikienė, R., V. Tomkutė, Z. Kuodis, G. Niaura, and A. Malinauskas. 2007. Raman spectroelectrochemical study of polyaniline and sulfonated polyaniline in solutions of different pH. *Vib. Spectrosc.* 44:201–208. doi:10.1016/j.vibspec.2006.09.005

[41] Agosti, E., M. Rivola, V. Hernandez, M. Del Zoppo, and G. Zerbi. 1999. Electronic and dynamical effects from the unusual features of the raman spectra of oligo and polythiophenes. *Synth. Met.* 100:101–112. doi:10.1016/S0379-6779(98)00167-2

[42] Šetka, M., R. Calavia, L. Vojkůvka, E. Llobet, J. Drbohlavová, and S. Vallejos. 2019. Raman and XPS studies of ammonia sensitive polypyrrole nanorods and nanoparticles. *Sci. Rep.* 9:1–10. doi:10.1038/s41598-019-44900-1

[43] Raj, R. P., P. Ragupathy, and S. Mohan. 2015. Remarkable capacitive behavior of a Co 3 O 4–polyindole composite as electrode material for supercapacitor applications. *J. Mater. Chem. A.* 3:24338–24348. doi:10.1039/C5TA07046E

[44] Liu, Y. C., B. J. Hwang, W. J. Jian, and R. Santhanam. 2000. Santhanam, in situ cyclic voltammetry-surface-enhanced raman spectroscopy: studies on the doPIng–undoPIng of polypyrrole film. *Thin Solid Films* 374: 85–91. doi:10.1016/S0040-6090(00)01061-0

[45] Nemade, K. R., and S. A. Waghuley. 2013. UV–VIS spectroscopic study of one pot synthesized strontium oxide quantum dots. *Results Phys.* 3:52–54. doi:10.1016/j.rinp.2013.03.001

[46] Toufiq, A. M., F. Wang, Q. U. A. Javed, Q. Li, and Y. A. N. Li. 2013. Photoluminescence spectra and magnetic properties of hydrothermally synthesized MnO 2 nanorods. *Mod. Phys. Lett. B.* 27:1350211. doi:10.1142/S0217984913502114

[47] Sherin, J. S., J. K. Thomas, and S. Manoj. 2015. Facile synthesis and characterization of pyrolusite, *β*-MnO2, nano crystal with magnetic studies. *Int. J. Sci. Eng. Appl.* 4:250–252. doi:10.7753/IJSEA0405.1003

[48] Toufiq, A. M., F. Wang, Q-U-A Javed, Q. Li, and Y. Li. 2014. Hydrothermal synthesis of MnO 2 nanowires: structural characterizations, optical and magnetic properties. *Appl. Phys. A.* 116:1127–1132. doi:10.1007/s00339-013-8195-0

[49] Chatterjee, M. J., A. Ghosh, A. Mondal, and D. Banerjee. 2017. Polyaniline–single walled carbon nanotube composite–a photocatalyst to degrade rose bengal and methyl orange dyes under visible-light illumination. *RSC Adv.* 7:36403–36415. doi:10.1039/C7RA03855K

[50] Tripathi, A., S. K. Mishra, I. Bahadur, and R. K. Shukla. 2015. Optical properties of regiorandom polythiophene/Al 2 O 3 nanocomposites and their application to ammonia gas sensing. *J. Mater. Sci: Mater. Electron.* 26:7421–7430. doi:10.1007/s10854-015-3373-9

[51] Vanheusden, K., W. L. Warren, C. H. Seager, D. R. Tallant, J. A. Voigt, and B. E. Gnade. 1996. Mechanisms behind green photoluminescence in ZnO phosphor powders. *J. Appl. Phys.* 79:7983–7990. doi:10.1063/1.362349

[52] Vanheusden, K., C. H. Seager, W. L. Warren, D. R. Tallant, and J. A. Voigt. 1996. Correlation between photoluminescence and oxygen vacancies in ZnO phosphors. *Appl. Phys. Lett.* 68:403–405. doi:10.1063/1.116699

[53] Dey, S., and A. Kumar Kar. 2019. Morphological and optical properties of polypyrrole nanoparticles synthesized by variation of monomer to oxidant ratio. *Mater. Today: Proc.* 18:1072–1076. doi:10.1016/j.matpr.2019.06.566

[54] Nemade, K., P. Dudhe, and P. Tekade. 2018. Enhancement of photovoltaic performance of polyaniline/graphene composite-based dye-sensitized solar cells by adding TiO2 nanoparticles. *Solid State Sci.* 83:99–106. doi:10.1016/j.solidstatesciences.2018.07.009

[55] Kaempgen, M., C. K. Chan, J. Ma, Y. Cui, and G. Gruner. 2009. Printable thin film supercapacitors using single-walled carbon nanotubes. *Nano Lett.* 9:1872–1876. doi:10.1021/nl8038579

[56] Jaidev , R. I. Jafri, A. K. Mishra, and S. Ramaprabhu. 2011. Polyaniline–MnO2nanotube hybrid nanocomposite as supercapacitor electrode material in acidic electrolyte. *J. Mater. Chem.* 21:17601–17605. doi:10.1039/c1jm13191e

[57] Han, G., Y. Liu, L. Zhang, E. Kan, S. Zhang, J. Tang, and W. Tang. 2014. MnO2 nanorods intercalating graphene oxide/polyaniline ternary composites for robust High-Performance supercapacitors. *Sci. Rep.* 4: 4824–4830. doi:10.1038/srep04824

[58] Zhou, J., L. Yu, W. Liu, X. Zhang, W. Mu, X. Du, Z. Zhang, and Y. Deng. 2015. High performance all-solid supercapacitors based on the network of ultralong manganese dioxide/Polyaniline Coaxial Nanowires. *Sci. Rep.* 5:17858–17864. doi:10.1038/srep17858